Pneumatic bio-soft robot module: Structure, elongation and experiment

Bao Guanjun, Yao Pengfei, Xu Zonggui, Li Kun, Wang Zhiheng, Zhang Libin, Yang Qinghua*

(*College of Mechanical Engineering, Zhejiang University of Technology, Hangzhou 310014, China*)

Abstract: Soft robotics, often taking inspirations from biomimetics, is an exciting novel research field and has great capability to work with creatures. A new type of bio-soft robot inspired by elephant trunk and octopus was proposed, which has a promising application in robotic agricultural harvesting. The two modularized structures, basal segment and caudal segment, were elaborated in detail. They both have three side chambers and one central chamber, which are reinforced by springs for better stretch performance in axial direction without radial expansion. All the chambers can act as drivers when inflated with compressed air. More importantly, the central chamber was designed for regulating the stiffness of the robot module as needed in application. The primary static model for axial elongation was established for the fundamental analysis of the bio-soft robot module's features, such as iso-force, isobaric and isometric characteristics. Simulation and experimental results showed that the motion of the proposed bio-soft module has approximate linearity in iso-force and isobaric conditions, and strict linearity in isometric condition.

Keywords: bio-soft robot, pneumatic muscle actuator, static model, harvesting robot

DOI: 10.3965/j.ijabe.20171002.2909

Citation: Bao G J, Yao P F, Xu Z G, Li K, Wang Z H, Zhang L B, et al. Pneumatic bio-soft robot module: Structure, elongation and experiment. Int J Agric & Biol Eng, 2017; 10(2): 114–122.

1 Introduction

Traditional robots are widely used in industrial applications due to their outstanding advantages of high stiffness, strength, precision and operating speed. With the development of the economy and society, more fields are trying to use robot to work for or cooperate with human being. For example, in household service, handicap and aged assistance, agricultural automation, medical surgery and rehabilitation applications, robots can realize high quality performance with low cost, minimized manual work and decreased or even no harm to human health. In these unstructured environments, the operating subjects are too complex and/or changeable to be described by accurate mathematical models. While great efforts were devoted to apply rigid robots from industrial lines to these fields, the aforementioned advantages of traditional robots happened to be the constraint factors which lead to failure to accomplish such tasks. The above mentioned background arose the development and research on soft robotics[1,2]. To achieve the flexible capacity, several types of soft materials, such as silicon rubber[3], Shape Memory Alloy (SMA)[4,5] and Electroactive Polymers (EAP)[5,6], were employed to develop non-rigid or low-rigid robot structure. Driven by SMA, EAP, pneumatic or magnetorheological power, these soft robots feature sufficient flexibility, adaptability, hyper-redundant or infinite degree of freedom, which enabled them to

Received date: 2016-10-19 **Accepted date:** 2017-02-28

Biographies: Bao Guanjun, PhD, Associate Professor, research interests: mechatronics and robotics in agriculture, Email: gjbao@zjut.edu.cn; **Yao Pengfei**, Master, research interests: soft robotics, Email: yuitta@163.com; **Xu Zonggui**, Master, research interests: soft robotics, Email: 497670085@qq.com; **Li Kun**, Master, research interests: soft robotics, Email: 575088592@qq.com; **Wang Zhiheng**, PhD, Lecturer, research interests: robotics and intelligent equipment, Email: wzh232@zjut.edu.cn; **Zhang Libin**, PhD, Professor, research interests: robotics and intelligent equipment, Email: robot@zjut.edu.cn.

***Corresponding author: Yang Qinghua,** PhD, Professor, research interests: robotics and intelligent equipment. Mailing address: College of Mechanical Engineering, Zhejiang University of Technolgoy, No.18 of Chaowang Road, Hangzhou 310014, China. Tel: +86-571-88320819, Email: zjutme@163.com.

reshape their body and change the size as needed to adapt to the environment and subjects. They were preferred over rigid industrial robot for safe interaction with biological subjects and operation in unknown circumstances, and there is no need of advanced mathematical description or even awareness of the nature of their environments.

Generally, soft robots are inspired by natural creatures. It is common practice to study the structure and working principle of one species which shows unique features. Bionic robots are designed using soft materials and actuators to acquire particular performances for prescribed task or environment, such as elephant trunk manipulator[7-9], octopus robot[10,11], starfish[12,13], cow-nosed ray robot[14,15]. The bio-inspired robots have soft bodies, soft movements, soft and safe interaction with their environment, subjects and partners[16]. The bio-inspired robot with soft materials and characteristics was defined as bio-soft robot.

Silicon rubber is frequently adopted to construct a type of long cylinder arm-like robot, such as aforementioned elephant trunk manipulator and octopus, as well as Pneumatic Muscle Actuator (PMA)[17,18], Flexible Micro-Actuator (FMA)[19], Flexible Pneumatic Actuator (FPA)[20], soft surgical robot[21]. Most arm-like soft robots made of silicon rubber have only one chamber where compressed air or fluid can inflate and deflate, or driving cable can be installed. FMA has three pockets which enable its motion of elongation, bending and torsion. In spite of these outstanding works, the adaptive variable stiffness, one of the significant behaviors of bionic bodies, still cannot be simulated by current bio-soft robots.

In this research, a new type of bio-soft robot module was developed, which can realize adaptive variable stiffness by structure design and corresponding control. Firstly, the structure and work principle will unfold the primary idea, which is described in detail in Section 2. Elongation is the essential motion of bio-soft robot module and Section 3 gives the detailed information on mathematic modelling for axial stretching. Based on the static model for elongation, simulations are executed in Section 4 to analyze the iso-force, isobaric and isometric characteristics. Section 5 presents the experimental results and discussions. Finally, conclusions are drawn in Section 6.

2 Structure and working principle

The proposed pneumatic bio-soft robot modules are composed of silicon rubber and reinforcing springs. Two module structures, namely the basal segment and caudal segment, were designed for multiple segments robot assembly. As depicted in Figure 1, the basal segment includes the silicon rubber body and pipes. The cylindrical silicon rubber body consists of one central chamber, three side chambers and three tube channels for the pipes. In the transverse section, the side chambers and channels are evenly distributed with the same angular step of 120°. Enclosed and compressed air can inflate or deflate through the pipes in each of the central chamber and side chambers. To prevent radical expansion, springs are embedded in the endospore and exospore of the chambers. Thanks to its modular design, the basal segment of pneumatic bio-soft robot modules can be connected with each other in series, forming multiple segments arm-like bio-soft robot. All the pipes will go through the tube channels inside its previous segment. As shown in Figure 2, the caudal segment has almost the same structure, with the only difference of conical shape.

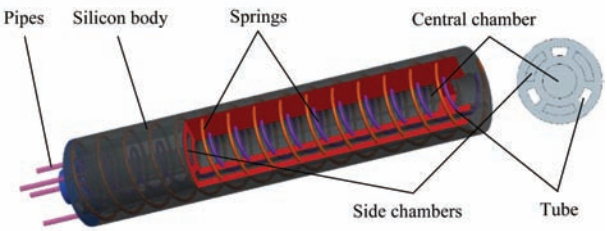

Figure 1 Structure of basal segment

Figure 2 Structure of caudal segment

When the side chambers are inflated with compressed air, the pneumatic bio-soft robot modules perform motion of elongation and bending, according to the air pressure controlling strategy. When arm-like robot is formed

using the basal segment and caudal segment, it will perform like the elephant trunk or octopus brachiopod, as shown in Figure 3.

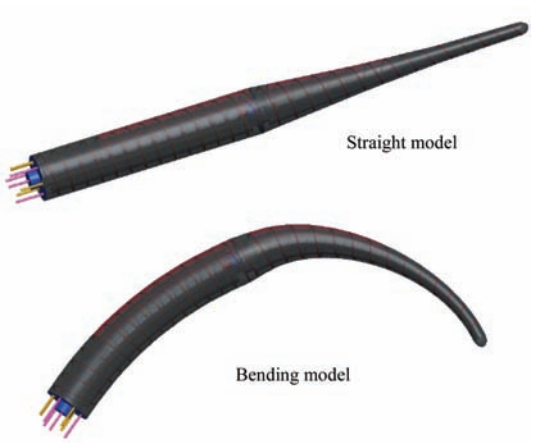

Figure 3 Arm-like soft robot formed by basal and caudal segment

3 Mathematical model for elongation

3.1 Axial static model for single chamber unit

Static forces acting on the separated single chamber unit of pneumatic bio-soft robot basal segment are depicted in Figure 4. According to the equilibrium of forces, the external force F can be calculated by:

$$F = F_p - F_a \tag{1}$$

where, F_p is the force on the chamber end produced by the differential air pressure between the atmosphere and chamber, MPa; F_a denotes the elastic force of the single chamber unit, N.

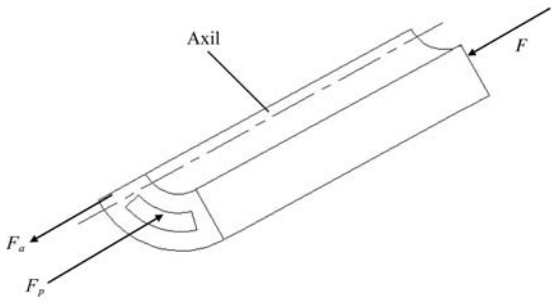

Figure 4 Force diagram of the single chamber unit

According to the meaning of F_p, it can be determined by the following formula:

$$F_p = pS_0 - p_{atm}S_0 \tag{2}$$

where, p is the air pressure inside the chamber, MPa; p_{atm} represents the atmospheric pressure, MPa; S_0 denotes the cross section area of the side chamber end, mm^2.

The transverse section of the pneumatic bio-soft robot basal segment is shown in Figure 5, where r_0, r_1, r_2, and r_3 are the outer circumference radius of the basal segment, the max radius and minimal radius of the side chamber and the radius of the central chamber, respectively. A_{r0} is the initial area of the isolated single chamber cross section. In this study, the above-mentioned radii have the following relations:

$$r_1 = 0.8r_0 \tag{3}$$

$$r_2 = 0.6r_0 \tag{4}$$

$$r_3 = 0.4r_0 \tag{5}$$

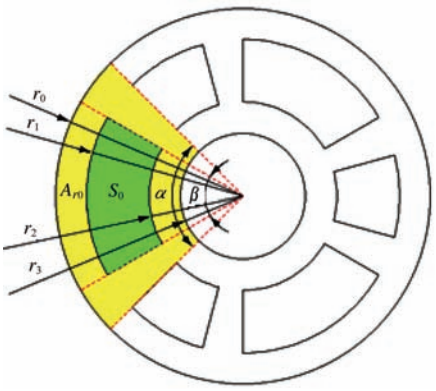

Figure 5 Transverse section of the basal segment

From the structural drawing of Figure 5, the cross section area of the side chamber end S_0 can be computed by

$$S_0 = \frac{r_1^2\beta}{2} - \frac{r_2^2\beta}{2} = \frac{(0.8r_0)^2\beta}{2} - \frac{(0.6r_0)^2\beta}{2} = 0.14r_0^2\beta \tag{6}$$

Substituting (6) into (2), we get

$$F_p = 0.14r_0^2\beta(p - p_{atm}) \tag{7}$$

The elastic force of single chamber unit F_a is the product of stress and its bearing area, as:

$$F_a = \sigma A_{rj} \tag{8}$$

where, A_{rj} represents the cross section area, mm^2; σ is the tensile stress of the isolated single chamber unit during elongation, MPa.

According to mechanics of materials, σ is defined as:

$$\sigma = E\varepsilon \tag{9}$$

where, E is the elasticity modulus of the material, MPa; ε denotes the strain of the isolated single chamber unit during stretch.

In the same way, ε is defined as:

$$\varepsilon = \frac{\Delta L}{L_0} \tag{10}$$

where, ΔL and L_0 are the stretched length and initial length of the isolated single chamber unit, respectively, mm.

In Figure 5, the central angle of the isolated single

chamber unit is α, and the initial area can be deduced as:

$$A_{r0}=\frac{r_0^2\alpha}{2}-\frac{r_3^2\alpha}{2}-S_0=0.42r_0^2\alpha-S_0 \tag{11}$$

Substituting Equation (6) into Equation (11), A_{r0} is simplified as:

$$A_{r0}=(0.42\alpha-0.14\beta)r_0^2 \tag{12}$$

Obviously, the volume of the isolated single chamber unit remains constant during motions. When inflated with compressed air, the chamber unit will elongate along the axis of the segment. Correspondingly, the thickness of all the walls of the structure will decrease. The volume of the isolated single chamber unit can be written as:

$$A_{r0}L_0=A_{rj}(L_0+\Delta L) \tag{13}$$

The formula can be rewritten to give the cross section area during motion:

$$A_{rj}=\frac{L_0}{L_0+\Delta L}A_{r0}=\frac{(0.42\alpha-0.14\beta)r_0^2L_0}{L_0+\Delta L} \tag{14}$$

Substituting Equations (9), (10) and (14) into Equation (8), the elastic force of single chamber unit is obtained:

$$F_a=\frac{(0.42\alpha-0.14\beta)Er_0^2\Delta L}{L_0+\Delta L} \tag{15}$$

Substituting Equations (9) and (15) into Equation (1), the static model for the isolated single chamber unit is:

$$F=0.14r_0^2\beta(p-p_{atm})-\frac{(0.42\alpha-0.14\beta)Er_0^2\Delta L}{L_0+\Delta L} \tag{16}$$

3.2 Axial static model of basal segment

Simultaneously inflating the three side chambers and central chamber of the basal segment with the same air pressure p will lead to its optimal elongation. The force equilibrium on the segment end is depicted in Figure 6, which also can be explained by the following equation:

$$\sum_{i=1}^{3}F_{pi}+F_{pm}=\sum_{i=1}^{3}F_{ai}+F \tag{17}$$

where, F_{pi} is the force produced by the side chamber unit i, N; F_{pm} denotes the force generated by the central chamber and F_{ai} represents the elastic force of the side chamber unit i, N.

Referring to Equation (7), the first term of Equation (17) is

$$\sum_{i=1}^{3}F_{pi}=3F_p=0.42(p-p_{atm})r_0^2\beta \tag{18}$$

The air pressures on the three side chambers' ends produce force $\sum_{i=1}^{3}F_{ai}$ as:

$$\sum_{i=1}^{3}F_{ai}=3F_a=\frac{(1.26\alpha-0.42\beta)Er_0^2\Delta L}{L_0+\Delta L} \tag{19}$$

The air pressure on the central chamber end produces force F_{pm} as:

$$F_{pm}=(p-p_{atm})\pi r_3^2=0.16(p-p_{atm})\pi r_0^2 \tag{20}$$

Substituting Equations (18), (19) and (20) into Equation (17), the expression of external loading F can be derived as:

$$F=\left[(0.42\beta+0.16\pi)(p-p_{atm})-\frac{(1.26\alpha-0.42\beta)E\Delta L}{L_0+\Delta L}\right]r_0^2 \tag{21}$$

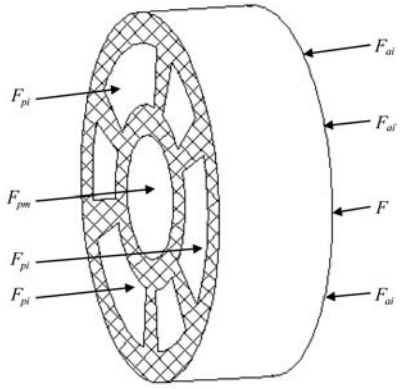

Figure 6 Force diagram of the basal segment end

4 Elongation simulation and analysis

Equation (21) represents the essential elongation model of the proposed pneumatic bio-soft robot module, which implies that the output force F is determined by the air pressure inside the chambers and the stretched length of the basal segment. Here, simulation based on Equation (21) was executed for further discussion and understanding of the static characteristics of the pneumatic bio-soft robot module. Specifications employed in the simulation are listed in Table 1.

Table 1 Specifications of the pneumatic bio-soft robot basal segment

Variable	Value
Initial length L_0/mm	110
Elastic module E/MPa	0.9
Radius r_0/mm	12
First central angle/rad	π/2
Second central angle/rad	π/3
Atmospheric pressure p_{atm}/MPa	0.1

4.1 Iso-force characteristic

Equation (21) can be rewritten into the following form to represent the relationship between p and ΔL when output force F is constant.

$$\Delta L=L_0\frac{50F-(8\pi+21\beta)r_0^2(p-p_{atm})}{(21\beta-8\pi)r_0^2(p-p_{atm})+(63\alpha-21\beta)Er_0^2-50F} \tag{22}$$

The simulated curves of stretched length with respect to internal air pressure for a series of constant output forces are shown in Figure 7. It is obvious that the stretched length will increase as the internal air pressure is raised. However, they are not in a strictly but approximately linear relationship, which can also be justified by Equation (22). Furthermore, when the output force is bigger, higher internal air pressure is expected to ensure the desired stretching length. Also, in this condition, the stretched length has much closer linear relationship to the internal air pressure.

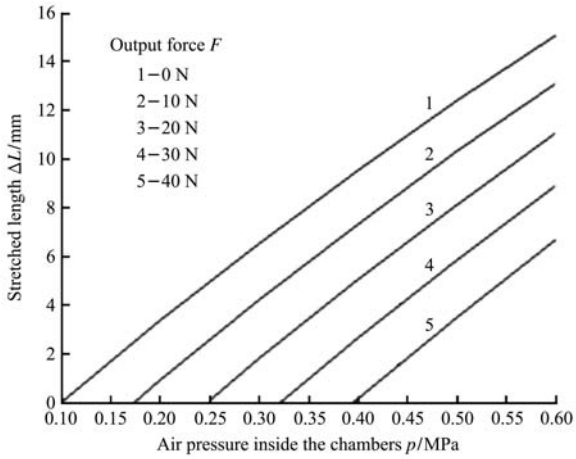

Figure 7 Iso-force curve of the basal segment

4.2 Isobaric characteristic

Equation (21) shows the relationship between output force F and stretched length ΔL, when internal air pressure p is constant. From the simulated curve shown in Figure 8, we can see that when the stretched length ΔL is smaller, the output force is relatively larger and F has better linearity with respect to ΔL. The stretched length ΔL reaches its maximum value while the output force is zero.

4.3 Isometric characteristic

If the stretched length ΔL is fixed, the output force F is expressed as a linear function of internal air pressure p by Equation (21). The shorter ΔL is, the less elastic force the segment body produces. Therefore, it is understandable that the bio-soft robot module will be more powerful if the stretched length ΔL is smaller, which is verified by the straight lines 1 to 5 in Figure 9.

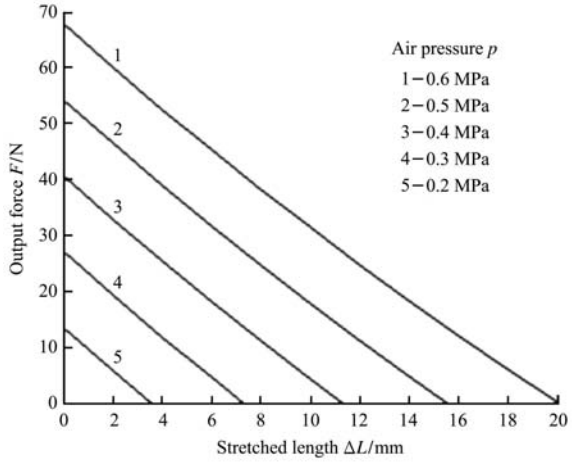

Figure 8 Isobaric curve of the basal segment

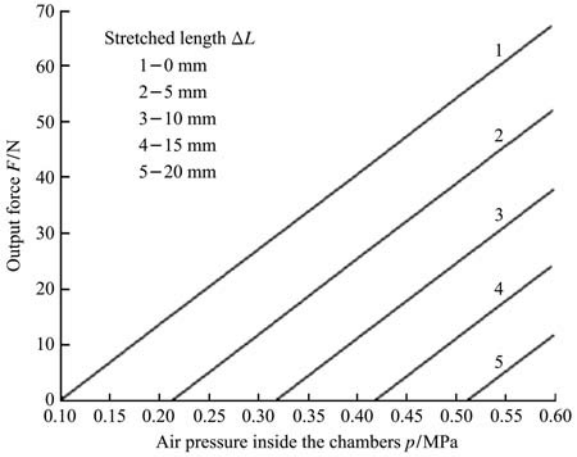

Figure 9 Isometric curve of the basal segment

5 Experimental results and discussion

5.1 Experimental bed

Experimental bed was developed based on the schematic diagram depicted in Figure 10, which is composed of the pneumatic bio-soft robot module prototype, compressed air source, data acquisition module and controlling module. Air pressure inside the robot prototype can be adjusted by the electro-pneumatic proportional valve supplied by the compressed air tank through relief valve and oil-mist separator. The controlling module will regulate the outlet pressure of the electro-pneumatic proportional valve, sample the data of displacement and output force of the robot prototype from sensors pre-treated by the STM32 microprocessor. The data acquisition, storing and processing software was

developed in the Microsoft Visual Studio environment. The experimental bed is shown in Figure 11. The instruments used and their specifications are listed in Table 2.

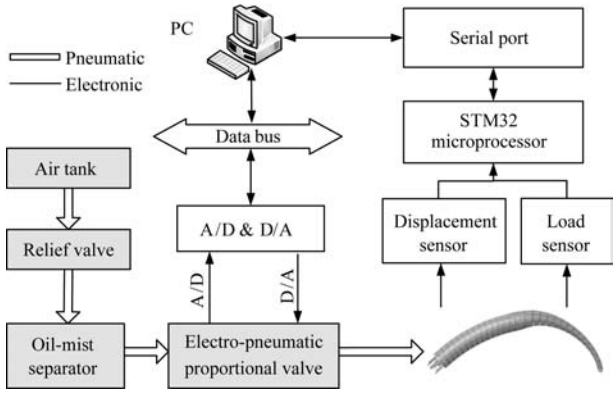

Figure 10 Schematic diagram of experiment bed

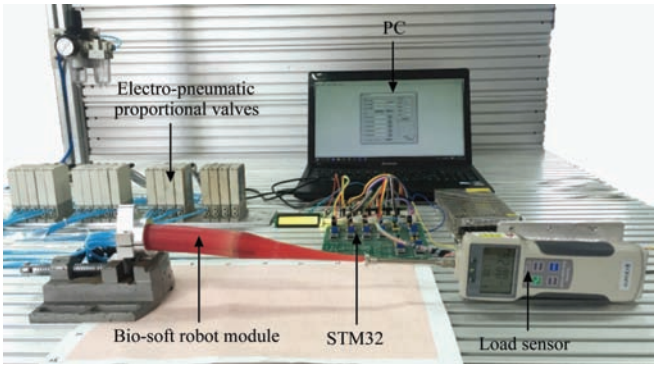

Figure 11 Experimental bed

Table 2 List of instruments for characteristics testing bed

Name	Type	Manufacturer
Relief valve	AW20-02G	SMC, Japan
Oil-mist separator	AFM20-02	SMC, Japan
Electro-pneumatic proportional valve	ITV0050-3BS	SMC, Japan
Displacement sensor	NS-WY06	Shanghai TM Automation Instruments
Load sensor	ZP-50	Shenzhen Aibao Instrument
DAQ card	STM32L4-Discovery	ST Microelectronics
PC	Thinkpad E420	Lenovo

5.2 Experimental data

5.2.1 Axial elongation with free end

The three side chambers and central chamber of the robot prototype were inflated with the same pressurized air to test the free end stretching ability. The air pressure ranges from 0.11 to 0.40 MPa with increment of 0.01 MPa. For each air pressure, displacement of the free end was sampled 10 times and the mean of them was taken as the measured value. The experimental data were accompanied by the simulated curve in Figure 12. The compatibility of the two curves implies that the established mathematical model can convey the static axial elongation property.

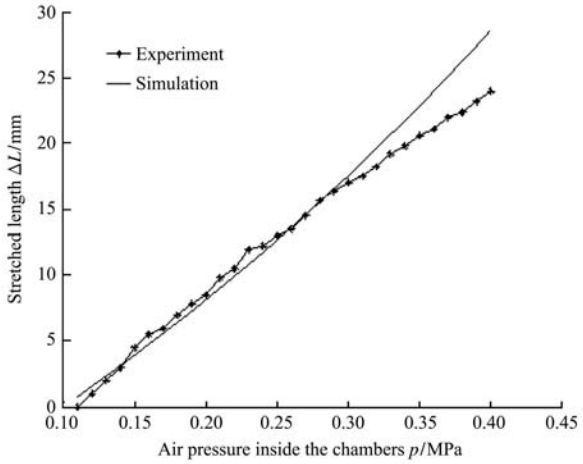

Figure 12 Experimental data and simulation curve of axial elongation without load

5.2.2 Isometric experiment

The isometric experiments were carried out with predetermined stretched length of the robot prototype. The comparison of experimental data and simulated curve, which proved the validity of the developed mathematical model for the pneumatic bio-soft robot basal segment, is shown in Figure 13.

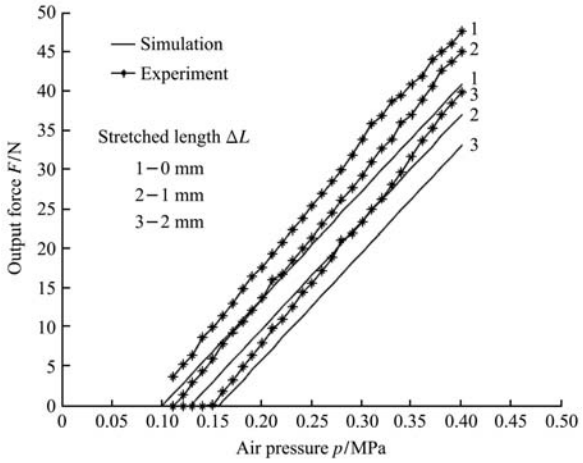

Figure 13 Simulation curve and experimental data for isometric characteristic

5.3 Discussion

5.3.1 Linearity

In controlling practice, especially for high speed applications, the linearity of the mathematical model of the controlled object and process are significantly desired for low algorithmic complexity and computing load. Referring to Equation (21), the output force F of the pneumatic bio-soft robot basal segment is proportional to the air pressure p inside its chambers. Obviously, the

F-*p* relationship is linear, which is also demonstrated by the simulation and experimental results shown in Figure 13. However, the ΔL-*p* and *F*-ΔL curves do not follow the linear relationship, as described and discussed in Section 4.1 and 4.2. The preferable means to achieve better linearity comes from the relatively higher load on the free end shown in Figure 7 or lower internal air pressure shown in Figure 8. The rubber body of basal segment should obey the Hooke's Law, which is a typical linear equation. The physical model changes due to the enclosed chambers with compressed air. High internal air pressure will increase the elastic module of the compressed air, which enhance its contribution to the basal segment elastic module *E*. In other words, the combined elastic module *E* of the basal segment has high tendency to vary during its motion, which leads to the change of correspondence between *F* and ΔL.

5.3.2 Error and compensation

In Figure 13, the experimental data shows the approximate linearity of the output force tendency over internal air pressure under different predetermined stretched lengths. Also the experimental data keeps the compatible trend with the simulated curve from theoretical model, with relatively bigger slopes. Nevertheless, there exist some deviation between the simulated data and the experimentally measured ones. The error increases with the internal air pressure. The reasonable cause for this phenomenon lies in the fact that when the chambers are inflated with compressed air, the viscous force inside the silicon rubber will shrink gradually to zero due to the inherent hysteresis of rubber material. The decreasing viscous force will convert the holding force produced by compressed air into output force. Also, as discussed above, the elastic module of the basal segment will change during its motion because of the compressed air inside the chambers and the transforming of its shell thickness. The theoretical model employs the constant value 0.9 MPa for the elastic module, which was measured for the pure silicon rubber used in the experiment. As the actual elastic module may change during the robot module's motion, the fixed constant elastic module is one of the factors causing the deflection of simulated curve over actual experiment. In spite of the errors, the theoretical model can meet the requirement of application even without compensation, since the flexible body of the bio-soft robot can adapt itself to the environment and subject, decreasing or even eliminating the deviations. This is one of the significant advantages of bio-soft robot over traditional rigid structures.

5.3.3 Generality of the structure and static model

Two modules of the proposed pneumatic bio-soft robot have been discussed. And most of the work was devoted to the basal segment. The caudal segment appeared in Section 2 just to show its structure and application in the bio-soft robot assembly. The reason behind this is that the caudal segment has almost the same mechanical structure as the basal segment. The only difference of cone shape does not lead to complex modification of concept or mechanical design. The generality of the bio-soft robot modules makes it easy to design, revise the segments, and easy to construct arm-like bio-soft robot with needed segments combination.

As for the static model for elongation, simulation was done for iso-force, isobaric and isometric characteristics. Although only the axial free stretching and isometric experiment were carried out to prove the theoretical work, the compatibility between experimental data and simulated curve ensures the acceptable conclusion that the theoretical model is validated since all the feature analysis are based on the same elongation model expressed by Equation (21) or its variety.

5.3.4 Promising application in harvesting robot

It is well known that most of the agricultural fruits are crisp and should be harvested with great care to avoid damage on their body and surface. Conventional rigid robotic end-effectors can hardly find their way in this field. Scientists and engineers had tried several soft structures actuated by pressurized air for fruit harvesting effectors, such as cucumber and apple harvesting hands with flexible pneumatic actuator[22,23], fruit harvesting continuum manipulator with series flexible pneumatic actuator[24], soft robotic grippers for biological sampling[25], life-sized hand with printable soft actuators for cones holding[26]. These fruits harvesting or

collecting robotic end-effectors employed silicon rubber or similar soft materials and were actuated by flexible power source compressed air. They could reshape themselves to actively adapt to the grasping objects, minimizing the grasping stress. While for the relatively heavy and soft fruits, like pasta tomatoes and mango, the aforementioned end-effectors may not supply enough holding force just from shape-adapting locomotion. The grasping stress will increase greatly if the air pressure inside the actuator is enhanced at the holding state. In scenarios like this application, variable stiffness is preferred, which is the outstanding advantage of the proposed pneumatic soft robot module. The stiffness can be controlled as needed just by regulating the air pressures inside the three side chambers and central chamber. More specifically, the hand fingers or grippers can improve their stiffness to support the holding and operating at the grasping state without changing their shapes and over raising the contact stress with the fruits.

6 Conclusions

In this study, a new type of pneumatic bio-soft robot module was proposed and the contributions can be summarized as:

1) The novel bio-soft robot structure and working principle were developed. The bio-soft robot module is design into two basic forms: basal segment and caudal segment. The former is cylindrical and the latter is cone. Both of them are made of silicon rubber and have three side chambers and one central chamber.

2) As the preliminary mathematic fundamental, the axial elongation model was established. The typical axial stretching characteristics, such as iso-force, isobaric and isometric features, were analyzed via simulation.

3) The axial elongation model was verified by experiments. Also, the experimental curve implied the approximate linearity of the mathematic model. Errors were found in the experiments, and still the theoretical model can be applied even without compensation because of the flexible body of the bio-soft robot.

The work described here is just the initial phase of our research. The axial elongation model gives the theoretical basis for further study and application. In the future, to thoroughly investigate the nature, working principle, properties and performance of the pneumatic bio-soft robot modules, numerous efforts need to be devoted in directions of complete mathematical modeling, stiffness regulating, controlling, and interacting with environment and subjects. Only in this way can the proposed pneumatic bio-soft robot modules find their application in service, agriculture, or medical fields.

Acknowledgments

This study was financially supported by NSFC-Zhejiang Joint Foundation (Grant No. U1509212), National Natural Science Foundation of China (Grant No. 51405441, 51605434) and Natural Science Foundation of Zhejiang Province (Grant No. Q15E050025).

[References]

[1] Daniela R, Michael T. Design, fabrication and control of soft robots. Nature, 2015; 512(7553): 467–475.

[2] Fumiya I, Cecilia L. Soft robotics: challenges and perspectives. Procedia Computer Science, 2011; 7(29): 99–102.

[3] Elango N, Faudzi A M. A review article: investigations on soft materials for soft robot manipulations. International Journal of Advanced Manufacturing Technology, 2015; 80(5-8): 1027–1037.

[4] Villoslada A, Flores A, Copaci D, Blanco D, Moreno L. High-displacement flexible shape memory alloy actuator for soft wearable robots. Robotics and Autonomous Systems, 2015; 73SI: 91–101.

[5] Mao S X, Dong E B, Jin H, Xu M, Zhang S W, Yang J, Low K. Gait study and pattern generation of a starfish-like soft robot with flexible rays actuated by SMAs. Journal of Bionic Engineering, 2014; 11(3): 400–411.

[6] Mutlu R, Alici G, Xiang X C, Li W H. An active-compliant micro-stage based on EAP artificial muscles. Proceedings of 2014 IEEE/ASME International Conference on Advanced Intelligent Mechatronics, Besacon, France, 2014; pp. 611–616.

[7] Hannan M, Walker I D. Analysis and experiments with an elephant's trunk robot. Advanced Robot, 2001; 15(8): 847–858.

[8] Hannan M, Walker I D. Kinematics and the implementation of an elephant's trunk manipulator and other continuum style robots. Journal of Robot System, 2003; 20(2): 45–63.

[9] Shao T F, Zhang L B, Du M Y, Bao G J, Yang Q H. Fruit harvesting continuum manipulator inspired by elephant trunk.

Int J Agric & Biol Eng, 2015; 8(1): 57–63.

[10] Li T, Nakajima K, Kuba M, Gutnick T, Hochner B, Pfeifer R. From the octopus to soft robots control: an octopus inspired behavior control architecture for soft robots. Vie Et Milieu, 2013; 61(4): 211–217.

[11] Nakajima K, Hauser H, Li T, Pfeifer R. Information processing via physical soft body. Nature Scientific Report, 2015; 5(13): 10487.

[12] Otake M, Kagami Y, Inaba M, Inoue H. Motion design of a starfish-shaped gel robot made of electro-active polymer gel. Robot Autonomous Systems. 2002; 40(2-3): 185–191.

[13] Jin H, Dong E B, Mao S X, Xu M, Yang J. Locomotion modeling of an actinomorphic soft robot actuated by SMA springs. Proceedings of IEEE International Conference on Robotics & Biomimetics, Bali, Indonesia, 2014; pp.21–26.

[14] Suzumori K, Endo S, Kanda T, Kato N, Suzuki H. A bending pneumatic rubber actuator realizing soft-bodied manta swimming robot. Proceedings of International Conference on Robotics and Automation, Roma, Italy, 2007; pp.4975–4980.

[15] Cao Y, Bi S S, Cai Y R, Wang Y L. Applying central pattern generators to control the robotfish with oscillating pectoral fins. Industrial Robot: An International Journal, 2015; 42(5): 392–405.

[16] Pfeifer R, Lungarella M, Iida F. The challenges ahead for bio-inspired soft robotics. Communications of the Acm, 2012; 55(11): 76–87.

[17] Caldwell D G, Medrano-Cerda G A, Goodwin M J. Braided pneumatic actuator control of a multi-jointed manipulator. Proceedings of IEEE International Conference on Systems, Man and Cybernetics Proceedings, Le Touquet, France, 1993; pp. 423–428.

[18] Nuchkrua T, Leephakpreeda T. Fuzzy self-tuning PID control of hydrogen-driven pneumatic artificial muscle actuator. Journal of Bionic Engineering, 2013; 10(3): 329–340.

[19] Suzumori K, Iikura S, Tanaka H. Flexible microactuator for miniature robots. Proceedings of IEEE Micro Electro Mechanical Systems Conference, Nara, Japan, 1991; pp. 204–209.

[20] Yang Q H, Zhang L B, Bao G J, Ruan J. Research on novel flexible pneumatic actuator FPA. Proceedings of IEEE Conference on Robotics, Automation and Mechatronics, 2004; pp. 385–389.

[21] Zhang R X, Wang H S, Chen W D, Wang X Z. Motion analysis and experimental study of a cable-driven soft surgical robot. Proceedings of IEEE International Conference on Cyber Technology in Automation, Shenyang, China, 2015; pp. 2085–2090.

[22] Yang Q H, Jin Y D, Qian S M, Bao G J. Research on end-effector of apple picking based on new flexible pneumatic actuator. Transactions of the CSAM, 2010; 41(9): 154–158. (in Chinese)

[23] Zhang L B, Wang Y, Yang Q H, Bao G J, Gao F. Kinematics and trajectory planning of a cucumber harvesting robot manipulator. Int J Agric & Biol Eng, 2009; 2(1): 1–7.

[24] Shao T F, Zhang L B, Du M Y, Bao G J, Yang Q H. Fruit harvesting continuum manipulator inspired by elephant trunk. Int J Agric & Biol Eng, 2015; 8(1): 57–63.

[25] Galloway K C, Becker K P, Phillips B, J Kirby, Licht S. Soft robotic grippers for biological sampling on deep reefs. Soft Robotics, 2016; 3(1): 23–33.

[26] Niiyama R, Sun X, Sung C, An B, Rus D, Kim S. Pouch motors: printable soft actuators integrated with computational design. Soft Robotics, 2015; 2(2): 59–70.